

Supporting Information

**Theoretical investigation of the broad one-photon absorption line-shape of a flexible
symmetric carbazole derivative**

Yanli Liu,^{a,b} Javier Cerezo,^b Fabrizio Santoro,^{*b} Antonio Rizzo,^c Na Lin,^{*a} Xian Zhao^{*a}

^a *State Key Laboratory of Crystal Materials, Shandong University, 250100 Jinan, Shandong, PR China*

^b *CNR – Consiglio Nazionale delle Ricerche, Istituto di Chimica dei Composti Organo Metallici (ICCOM-CNR), Sede Secondaria di Pisa, Area della Ricerca, via G. Moruzzi 1, I-56124 Pisa, Italy*

^c *CNR – Consiglio Nazionale delle Ricerche, Istituto per i Processi Chimico Fisici (IPCF-CNR), Sede Secondaria di Pisa, Area della Ricerca, via G. Moruzzi 1, I-56124 Pisa, Italy.*

* Corresponding authors: fabrizio.santoro@iccom.cnr.it, linnakth@gmail.com, xianzhao@sdu.edu.cn

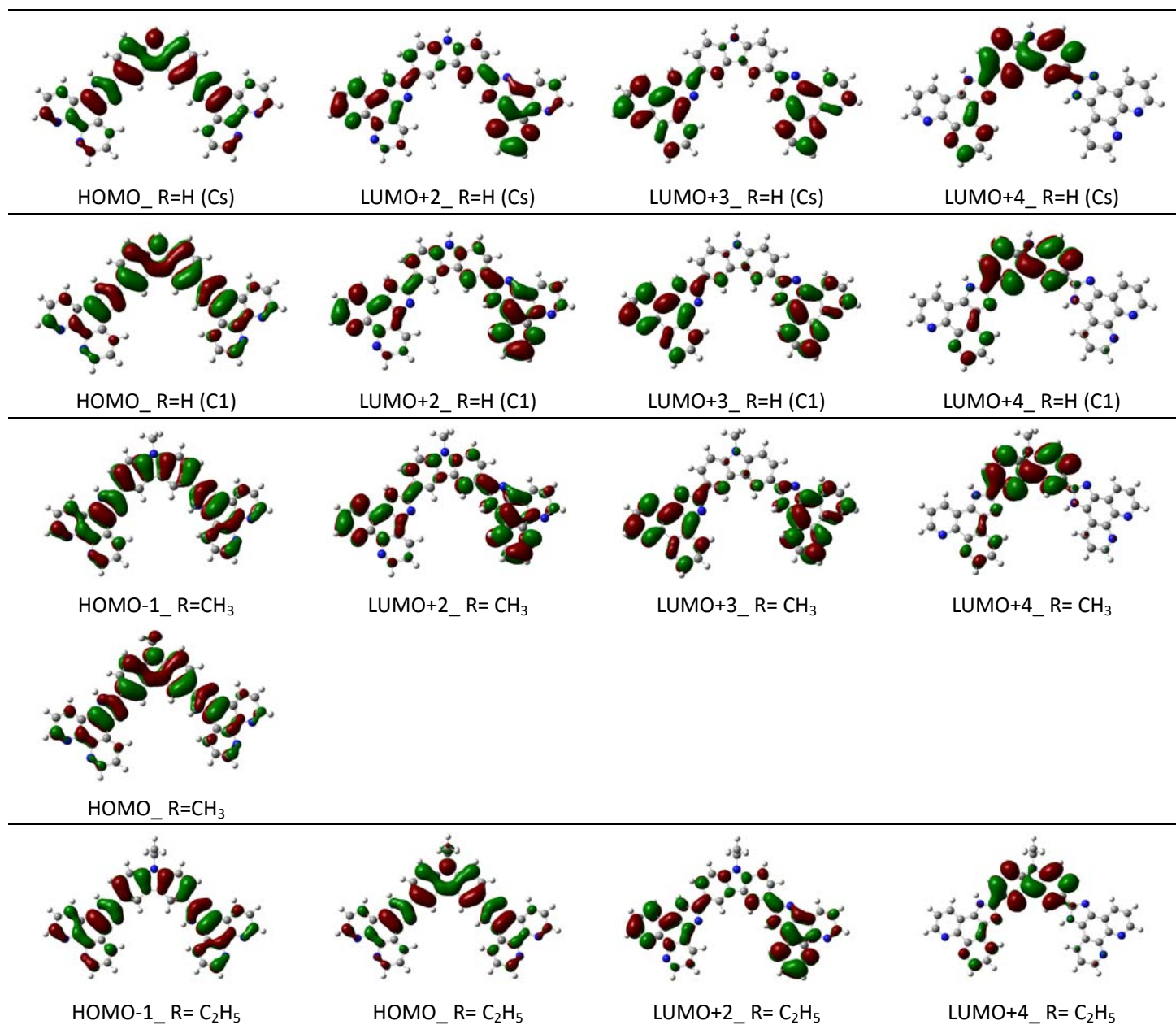


Fig. S1 *R-POCP*. The corresponding molecular orbitals of derivatives with R changing from H to C₂H₅

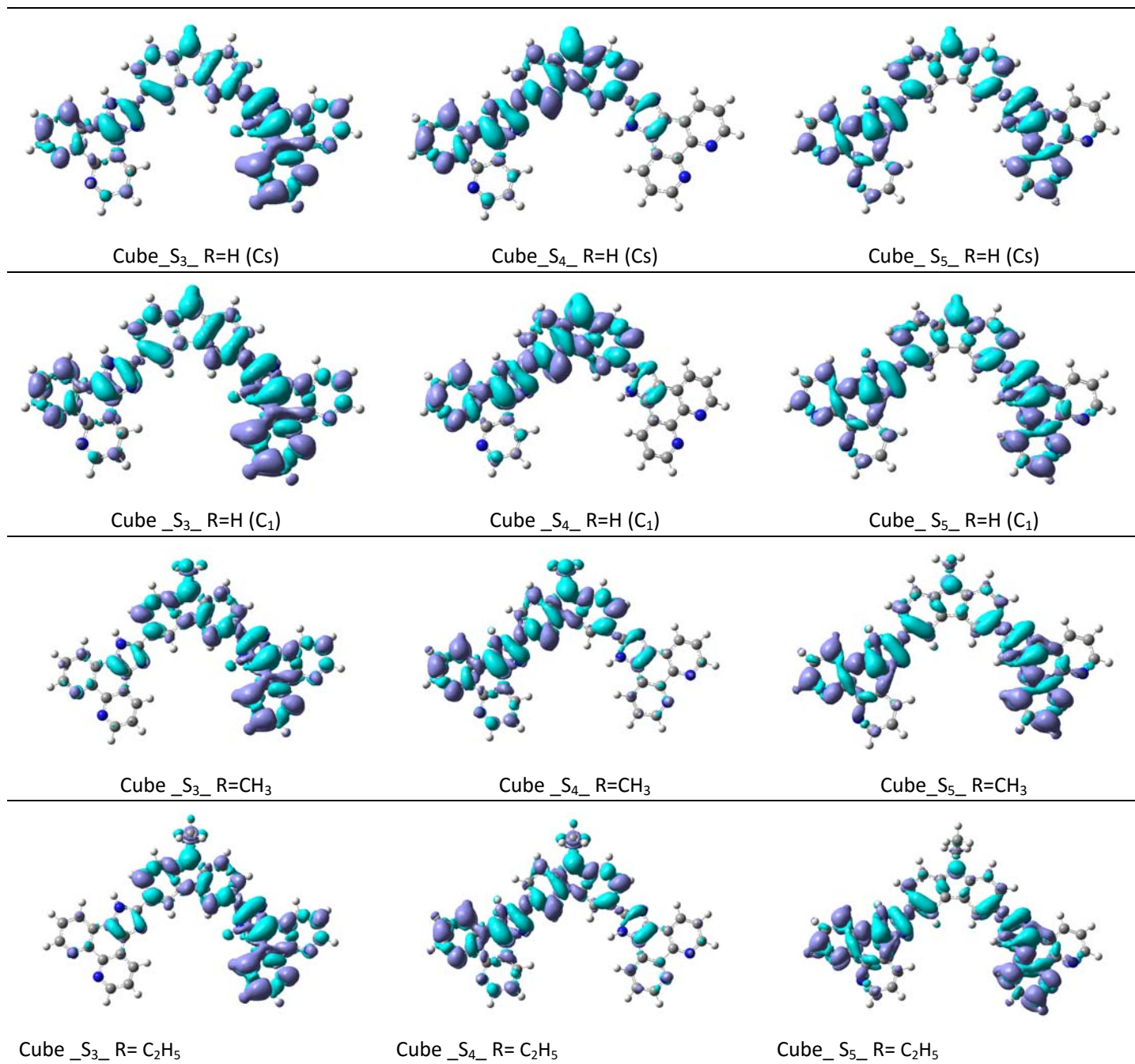


Fig. S2 R-POCP. Difference between the electronic densities of S_3 - S_5 and ground state of $R=H$, CH_3 and C_2H_5

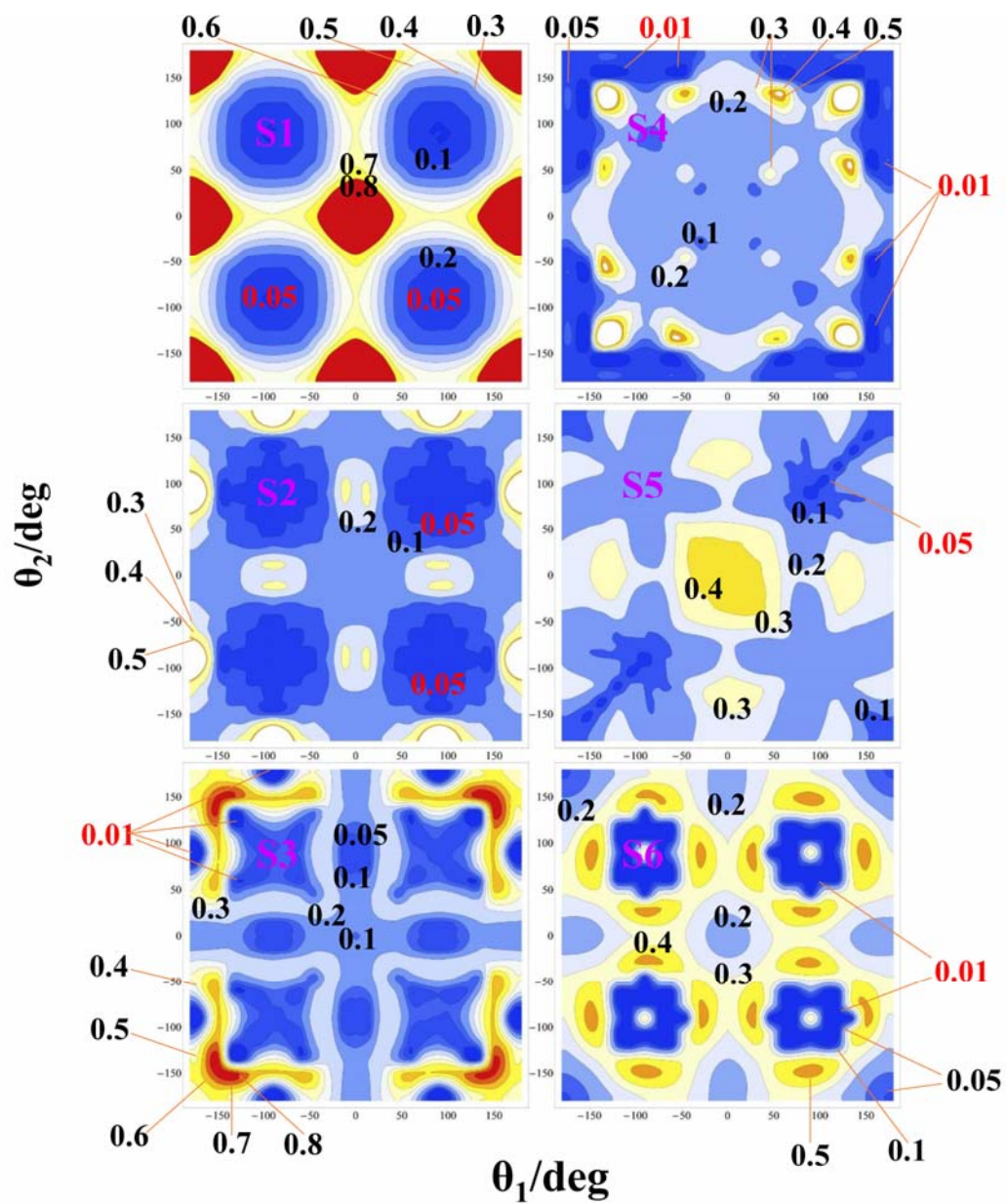


Fig. S3 H-POCP. ES relaxed scan as a function of the dihedral angles θ_1 and θ_2 , the oscillator strengths of the minima structure of each excited states are highlighted in red

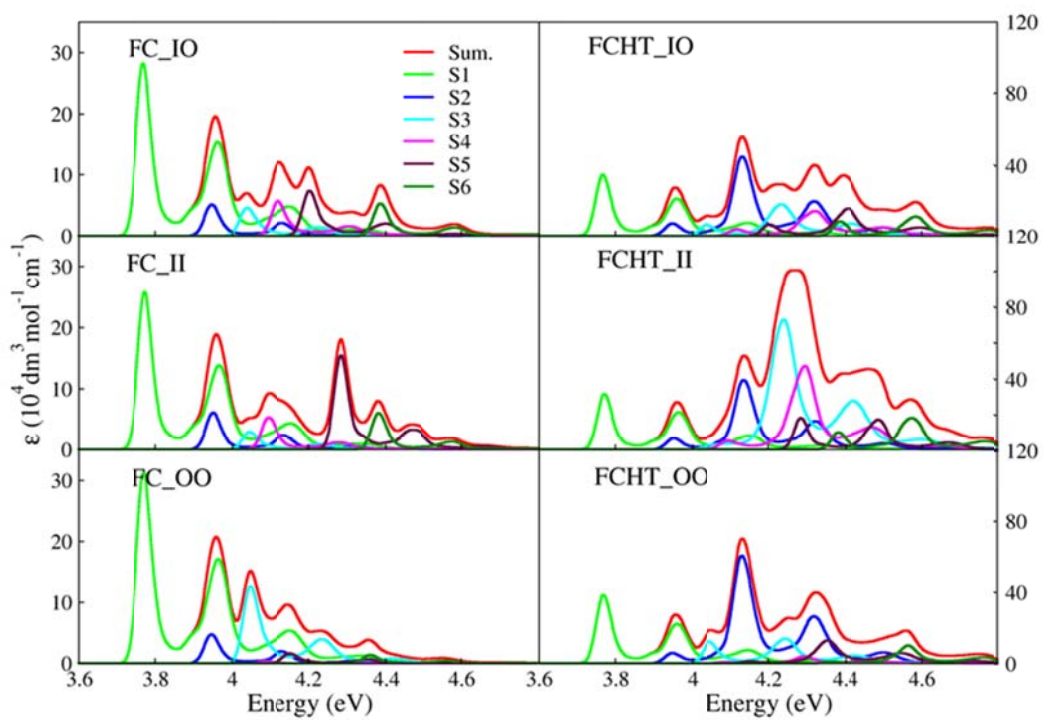


Fig. S4 H-POCP. Vibronic spectra computed with the TD approach at 0K for the first six excited electronic states of H-POCP excited states considering only the 196 fast r coordinates. Spectra convoluted with a Gaussian with HWHM=0.02eV.

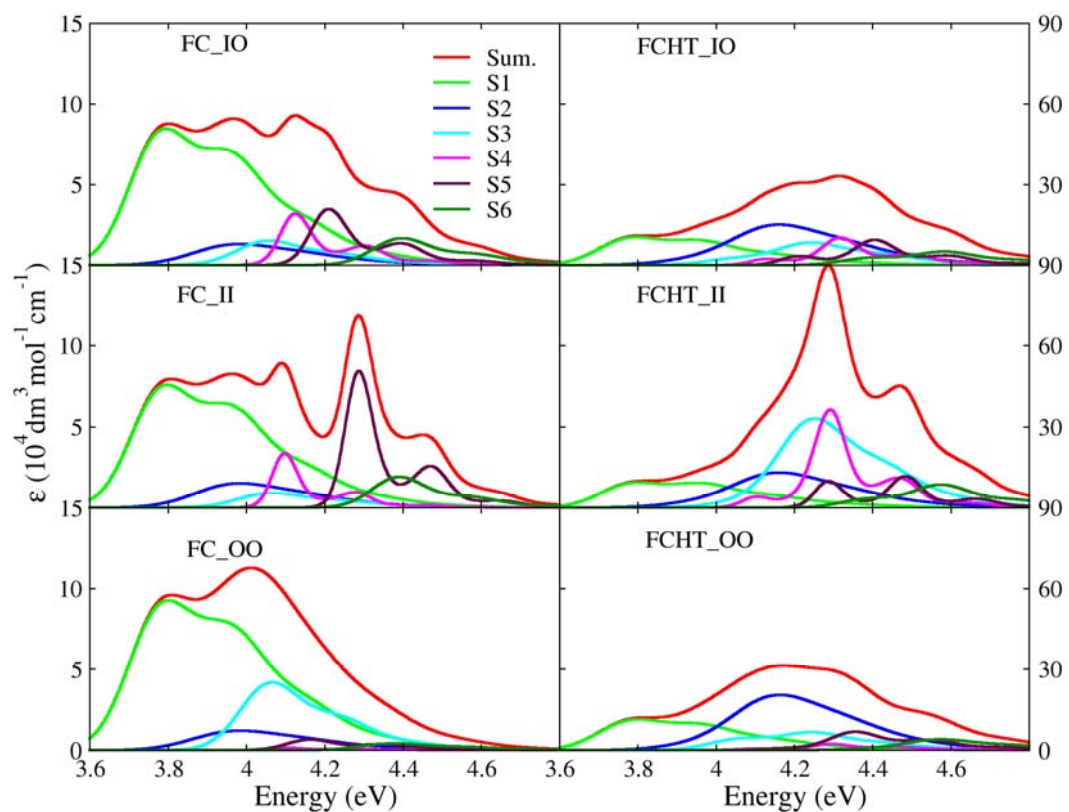


Fig. S5 H-POCP. Vibronic spectra computed with the TD approach at 300K for the first six excited electronic states of H-POCP excited states considering only the 196 fast r coordinates. Spectra convoluted with a Gaussian representing the solvent inhomogeneous broadening specific for each state of each conformer and reported in Table 2

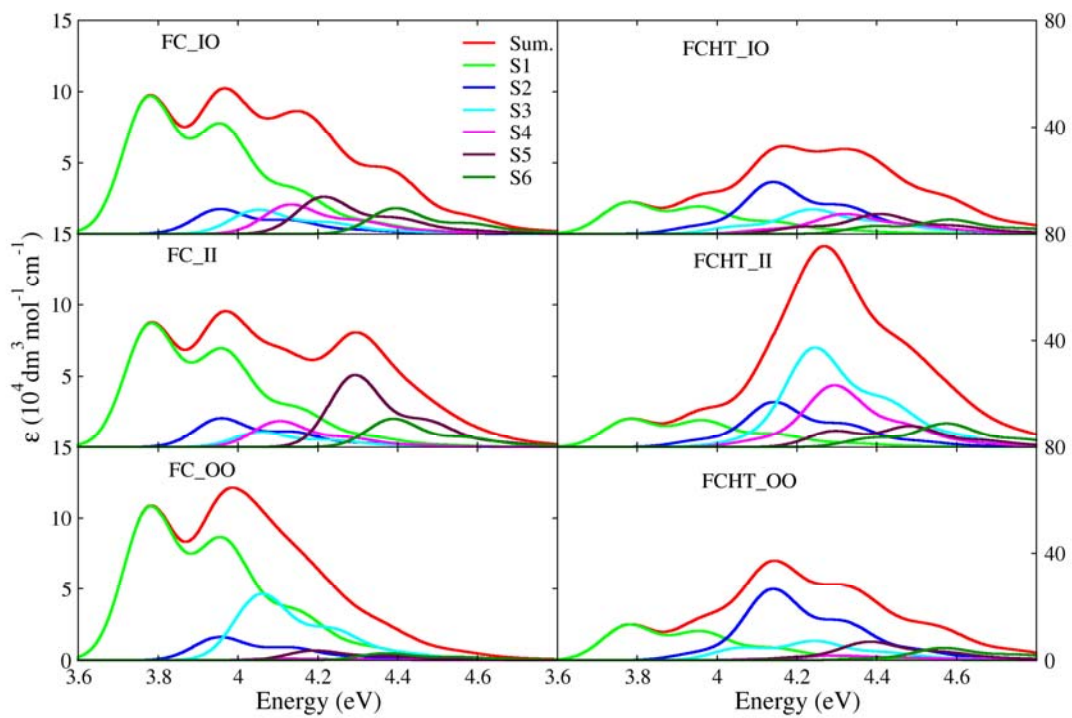


Fig. S6 H-POCP. Vibronic spectra computed with the TD approach at 300K for the first six excited electronic states of H-POCP excited states considering only the 196 fast r coordinates. Spectra convoluted with a Gaussian averaged solvent inhomogeneous broadening with HWHM of 0.07eV

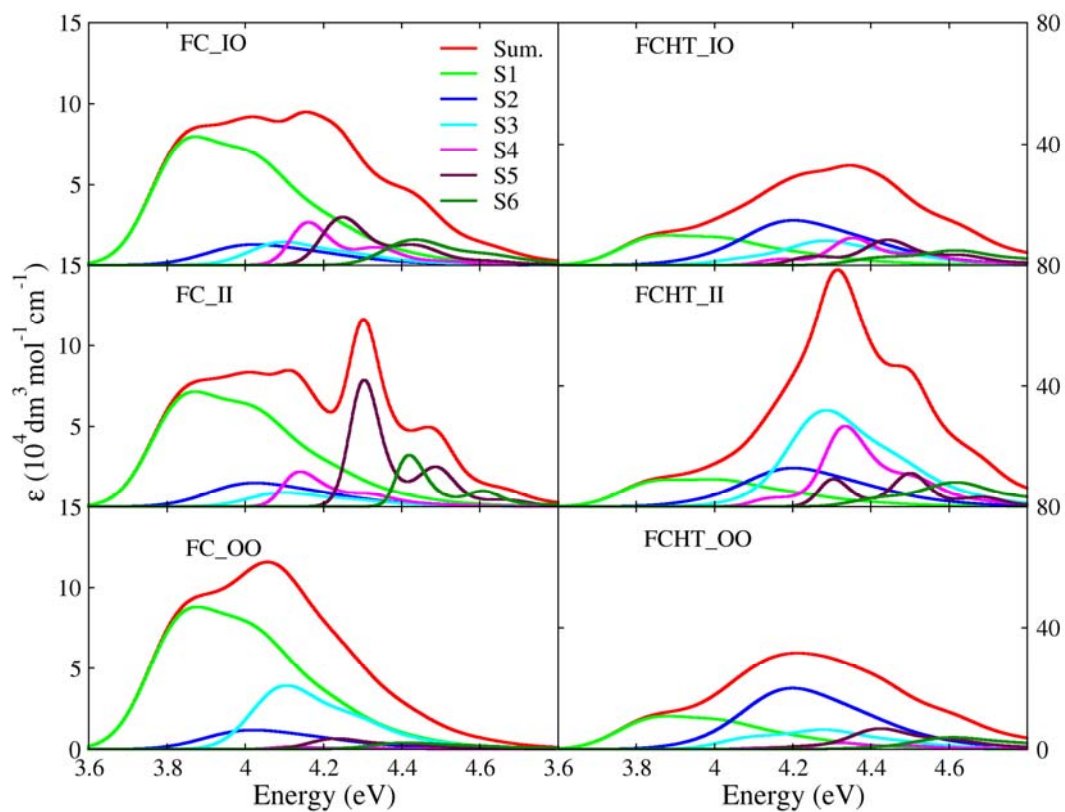


Fig. S7 H-POCP. FC and FCHT spectra obtained convoluting 196*FC/FCHT* spectra with torsional broadening of six excited states of three conformers of H-POCP, calculated at 300K. Spectra convoluted with a Gaussian representing the solvent inhomogeneous broadening specific for each state of each conformer and reported in Table 2

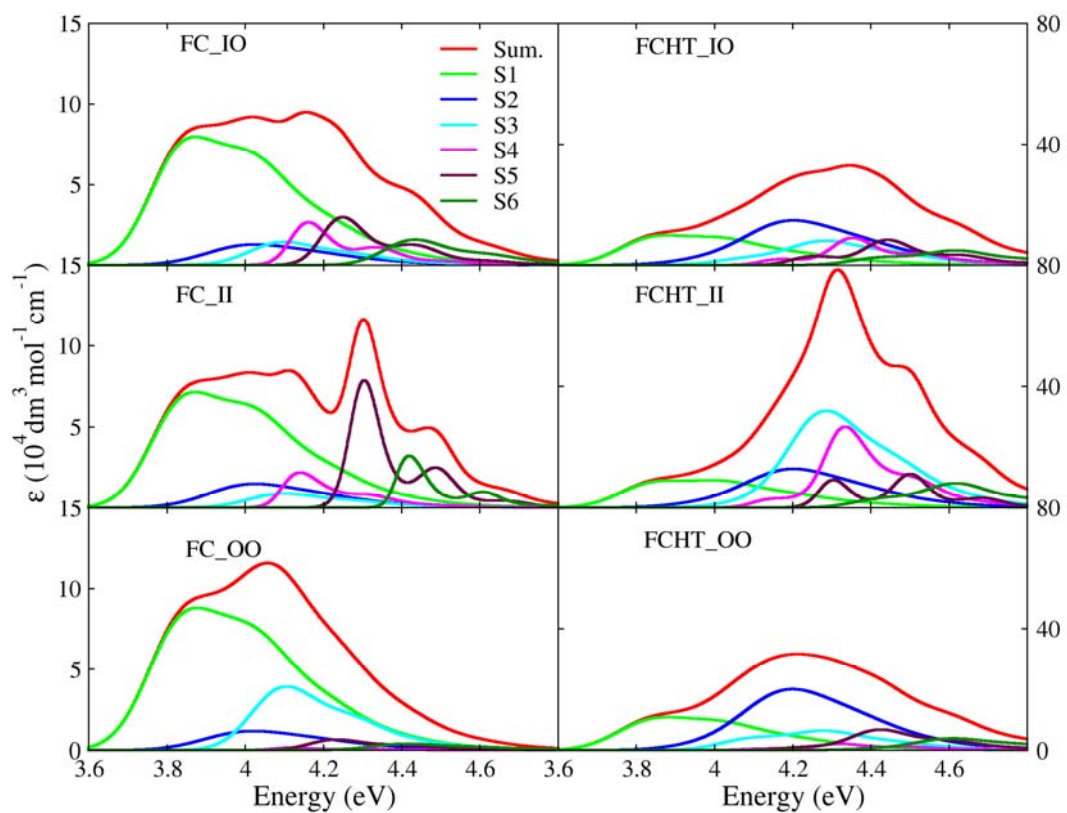


Fig. S8 H-POCP. FC and FCHT spectra obtained convoluting 196*FC/FCHT* spectra with torsional broadening of S_1 - S_6 of three conformers of H-POCP at 300K, convoluted with an averaged solvent broadening with HWHM of 0.07eV

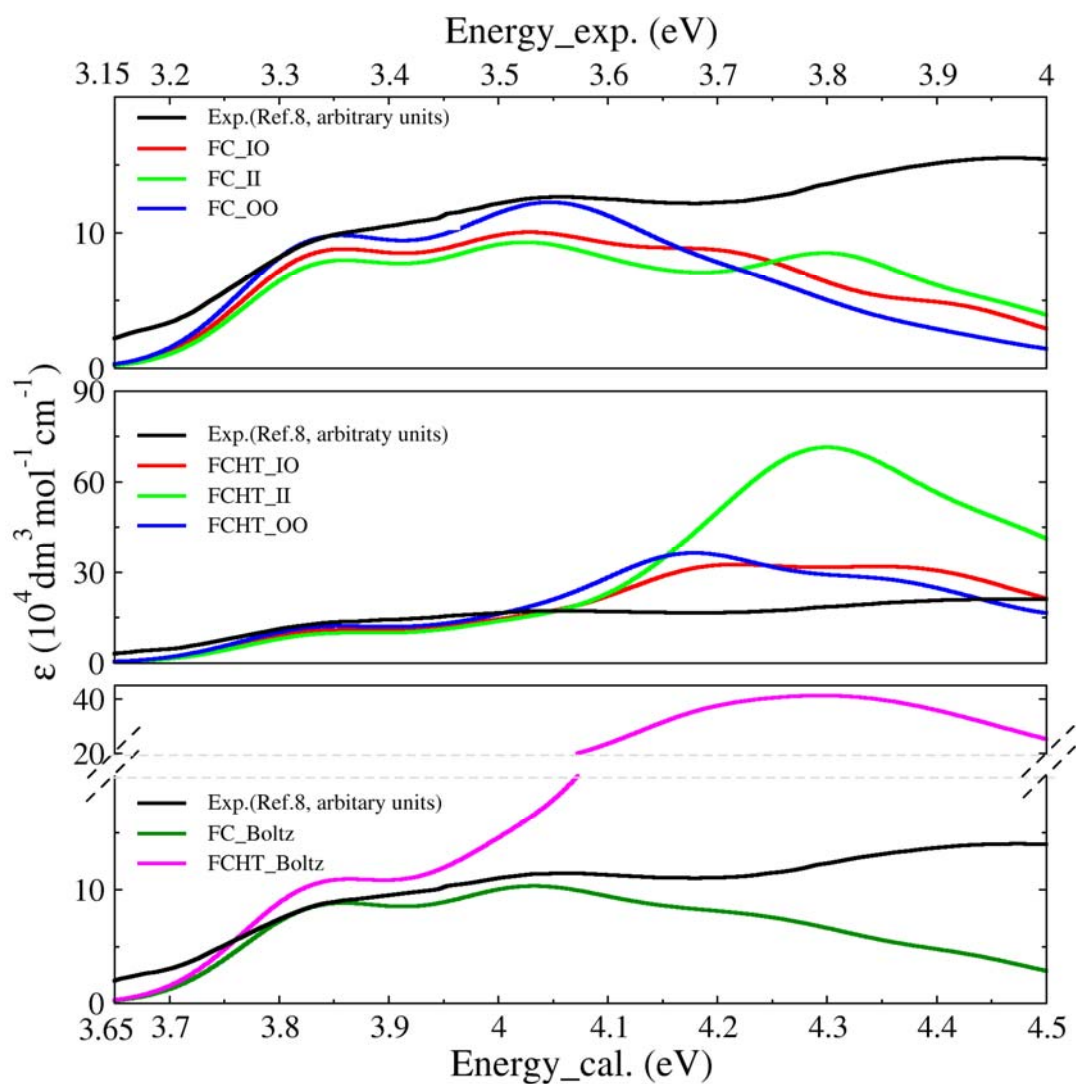


Fig. S9 H-POCP. Comparison of the experimental spectrum of POCP with the total FC and FCHT spectra computed for H-POCP by convoluting the histograms of the torsional broadening with the vibronic spectra at 300K, convoluted with an averaged solvent broadening with HWHM of 0.07eV

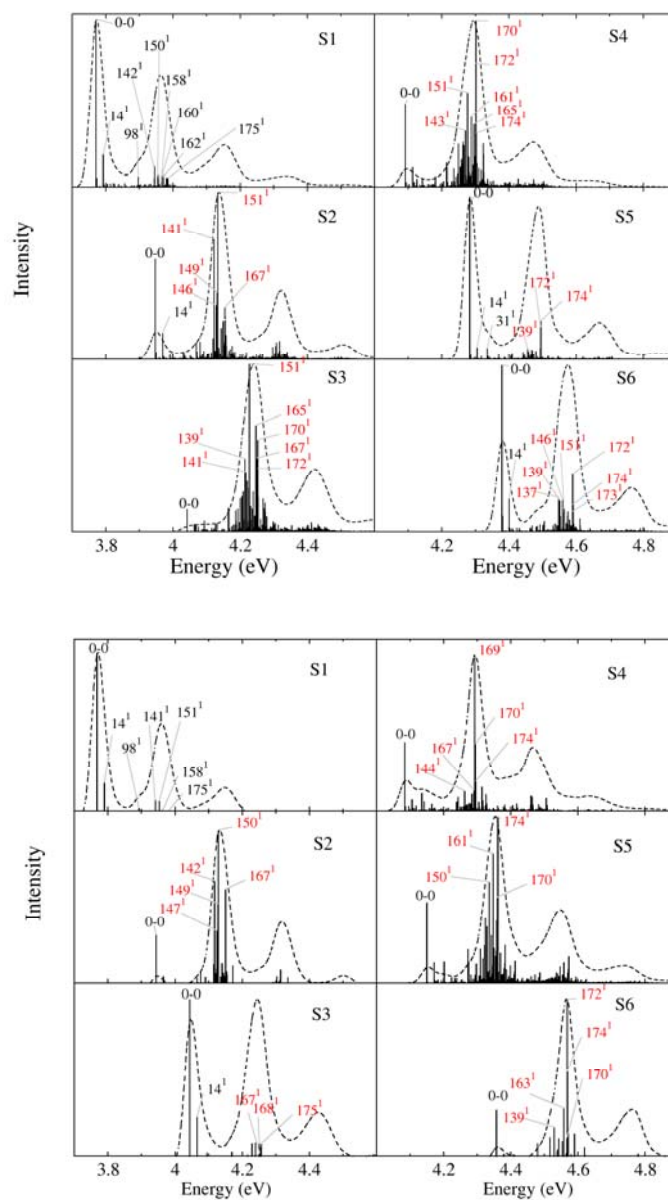


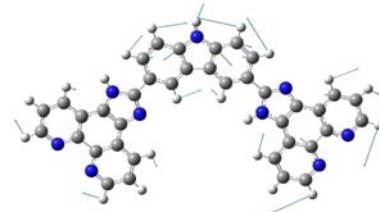
Fig. S10 H-POCP. Assignments of the main stick bands of the FCHT spectra of the S_1 - S_6 excited electronic states of conformers II (top) and OO (bottom). Vibrational contributions are labelled as " n^x ", where x indicates the quanta deposited on the excited-state normal mode n . Modes contributing most to HT are highlighted in red. Spectra are convoluted with a Gaussian spectral shape function with a HWHM of 0.02 eV. The convergence of the TI calculations for all the conformers, measured as the percentage of the recovered total intensity is always above 99 % for FC spectra and above 97.9% for FC+HT spectra



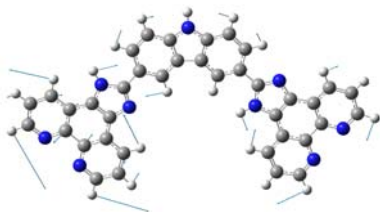
mode 14 (142.23 cm^{-1})



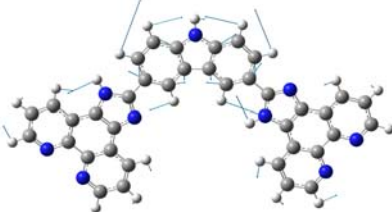
mode 98 (1000.61 cm^{-1})



mode 137 (1352.39 cm^{-1})



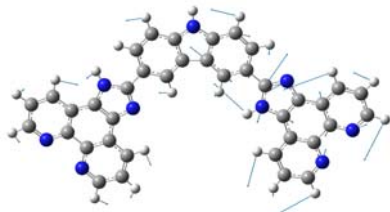
mode 138 (1354.38 cm^{-1})



mode 140 (1380.5 cm^{-1})



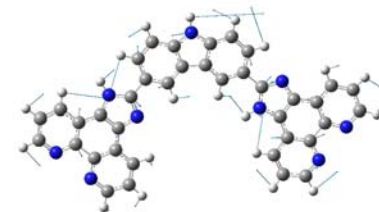
mode 141 (1389.80 cm^{-1})



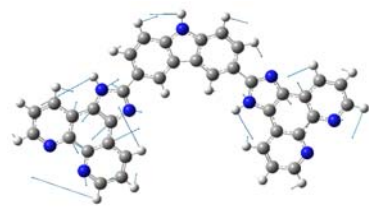
mode 146 (1450.25 cm^{-1})



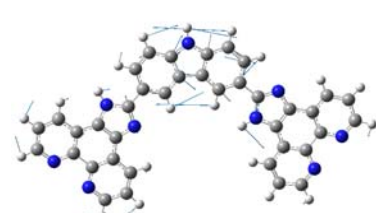
mode 148 (1459.57 cm^{-1})



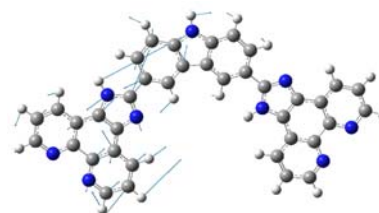
mode 149 (1461.82 cm^{-1})



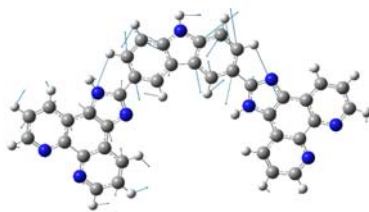
mode 151 (1538.02 cm^{-1})



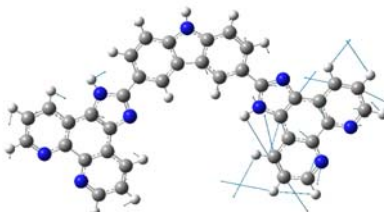
mode 158 (1538.02 cm^{-1})



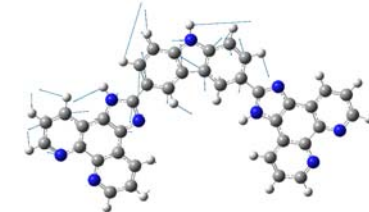
mode 164 (1617.33 cm^{-1})



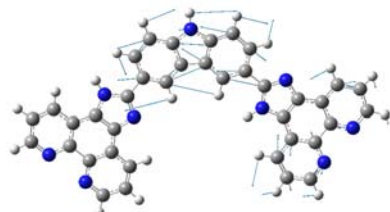
mode 168 (1662.10 cm^{-1})



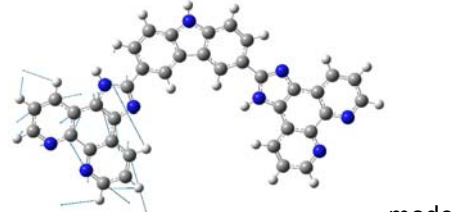
mode 170 (1671.31 cm^{-1})



mode 171 (1678.30 cm^{-1})

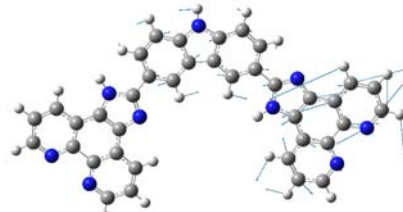


mode 172 (1696.00 cm^{-1})



mode 173 (1699.54 cm^{-1})

mode



mode 174 (1699.54 cm^{-1})

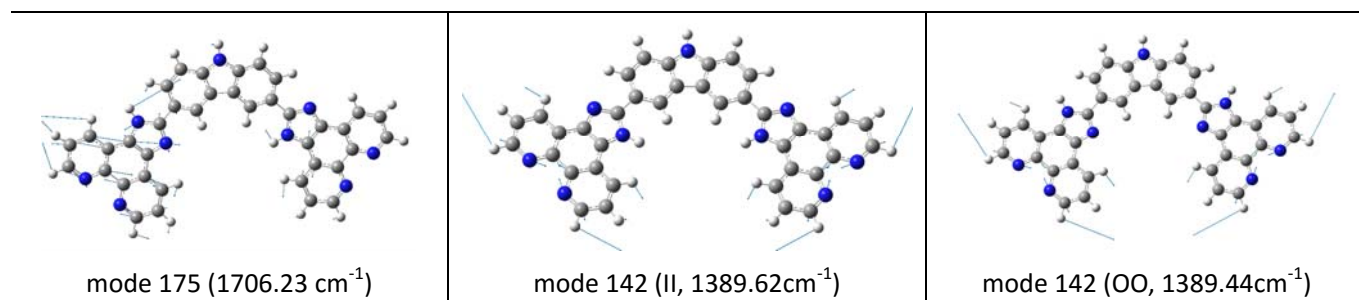
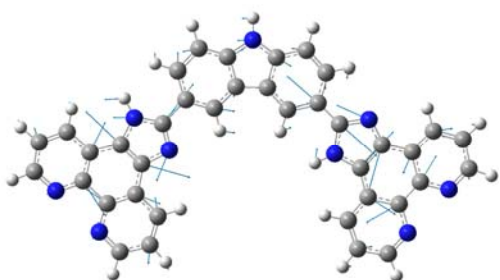
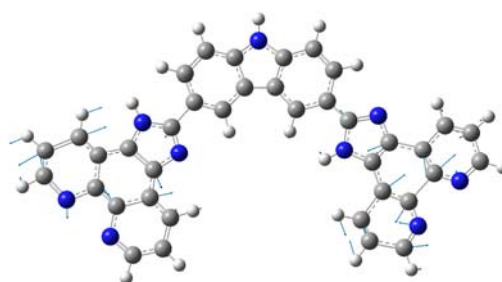


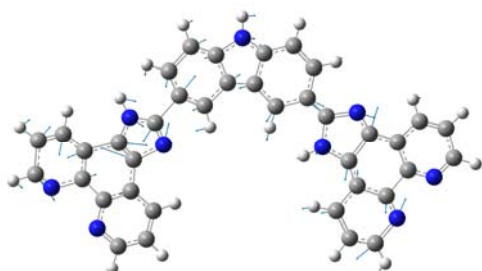
Fig. S11 H-POCP. Selected vibrational modes in Figure11, calculated for the ground electronic state at the CAMB3LYP/PCM/6-31G(d,p) level in DMF of IO conformer, frequencies are reported in parenthesis



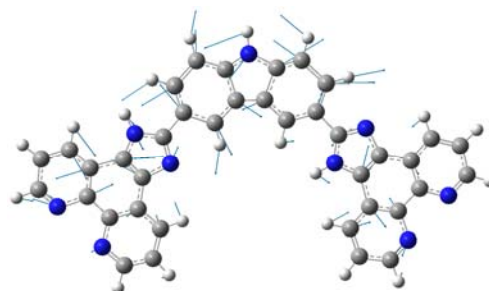
mode 1 (IO_S₁, 1846i)



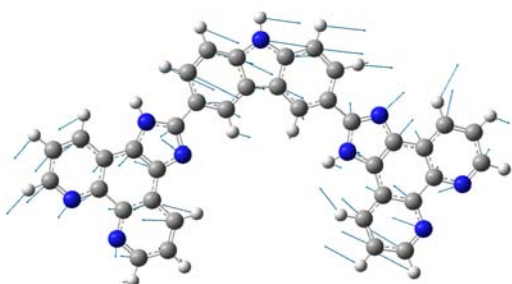
mode 1 (IO_S₂, 1051i)



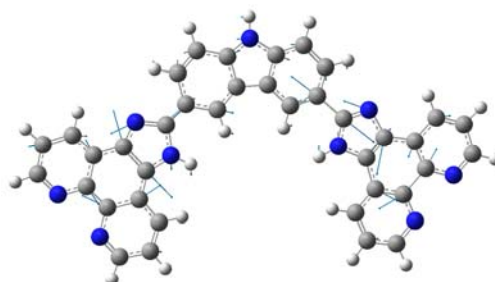
mode 1 (IO_S₃, 1119i)



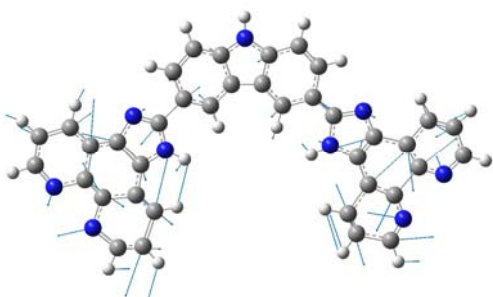
mode 1 (IO_S₄, 671i)



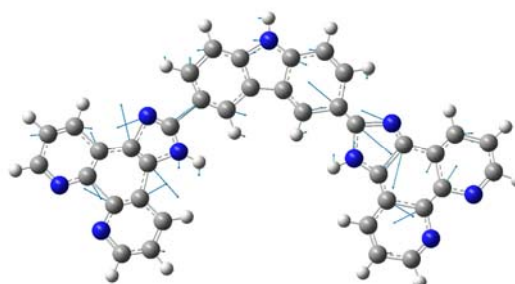
mode 1 (IO_S₆, 48i)



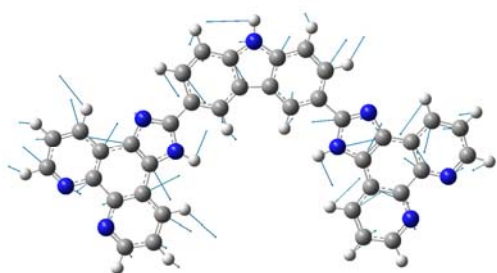
mode 1 (II_S₁, 1985i)



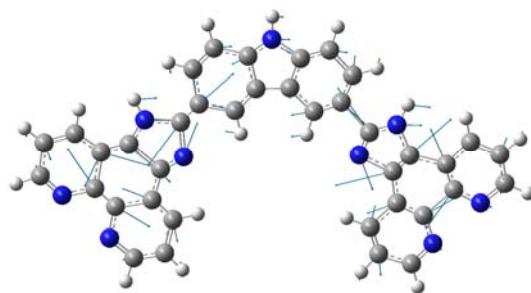
mode 1 (II_S₂, 941i)



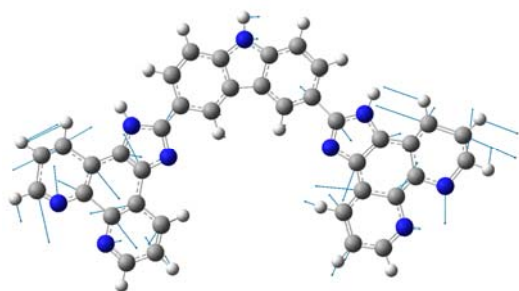
mode 1 (II_S₃, 3513i)



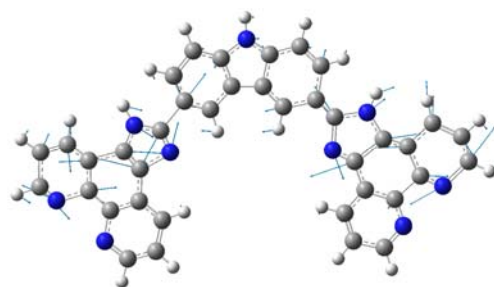
mode 1 (II_S₅, 454i)



mode 1 (OO_S₁, 1840i)



mode 1 (OO_S₂, 960i)



mode 1 (OO_S₃, 1260i)

Fig. S12 H-POCP. Selected vibrational modes highlighted in Table 3, calculated for the excited state at the ground state geometry at the CAMB3LYP/PCM/6-31G(d,p) level in DMF, frequencies are reported in parenthesis

Table S1: R-POCP N3-C5-C6-C7 (θ_1 , degree) and N4-C8-C9-C10 (θ_2 , degree) dihedral angles (See labels in Figure 1), oscillator strengths (δ_{OPA} , au), as well as transition energies (reported in parenthesis, eV) for the first ten excited states of carbazole analogues with R varying from H to C₈H₁₇, optimized at CAM-B3LYP/6-31G (d,p), in DMF.

R	θ_1	θ_2	S ₁	S ₂	S ₃	S ₄	S ₅	S ₆	S ₇	S ₈	S ₉	S ₁₀
H-Cs	-180	0	1.24 (3.92)	0.17 (4.05)	0.16 (4.13)	0.19 (4.21)	0.23 (4.29)	0.15 (4.47)	0.57 (4.64)	0.00 (4.65)	0.00 (4.65)	0.62 (4.69)
H-C ₁	-167.3	166.9	1.16 (3.95)	0.15 (4.06)	0.19 (4.15)	0.19 (4.22)	0.23 (4.30)	0.18 (4.48)	0.59 (4.65)	0.00 (4.65)	0.00 (4.65)	0.64 (4.72)
CH ₃	-167.3	167.0	1.23 (3.92)	0.16 (4.05)	0.04 (4.12)	0.22 (4.17)	0.33 (4.28)	0.11 (4.46)	0.67 (4.64)	0.00 (4.65)	0.00 (4.65)	0.68 (4.69)
C ₂ H ₅	-167.9	168.4	1.24 (3.91)	0.17 (4.05)	0.03 (4.11)	0.22 (4.16)	0.35 (4.28)	0.11 (4.46)	0.66 (4.63)	0.00 (4.65)	0.00 (4.65)	0.7 (4.69)
C ₂ H ₅ _{planar} ^a	180	180	1.29 (3.89)	0.19 (4.04)	0.02 (4.10)	0.19 (4.15)	0.36 (4.27)	0.10 (4.45)	0.08 (4.62)	0.00 (4.65)	0.00 (4.65)	0.68 (4.67)
C ₃ H ₇	-169.3	169.8	1.25 (3.91)	0.18 (4.05)	0.02 (4.11)	0.22 (4.16)	0.36 (4.27)	0.1 (4.45)	0.66 (4.62)	0.00 (4.65)	0.00 (4.65)	0.71 (4.68)
C ₄ H ₉	-171.4	172.0	1.27 (3.90)	0.18 (4.04)	0.02 (4.11)	0.21 (4.16)	0.36 (4.27)	0.1 (4.45)	0.65 (4.62)	0.00 (4.65)	0.00 (4.65)	0.71 (4.67)
C ₅ H ₁₁	-172.5	173.5	1.27 (3.90)	0.19 (4.04)	0.02 (4.10)	0.20 (4.15)	0.37 (4.27)	0.1 (4.45)	0.65 (4.62)	0.00 (4.65)	0.00 (4.65)	0.71 (4.67)
C ₆ H ₁₃	-166.2	-177.63	1.25 (3.90)	0.18 (4.05)	0.02 (4.11)	0.22 (4.16)	0.39 (4.27)	0.09 (4.45)	0.67 (4.63)	0.00 (4.65)	0.00 (4.65)	0.72 (4.68)
C ₇ H ₁₅	-166.6	-176.3	1.25 (3.90)	0.18 (4.05)	0.02 (4.11)	0.22 (4.16)	0.39 (4.27)	0.09 (4.45)	0.67 (4.62)	0.00 (4.65)	0.00 (4.65)	0.73 (4.68)
C ₈ H ₁₇	-164.3	-174.8	1.24 (3.91)	0.18 (4.05)	0.02 (4.11)	0.23 (4.16)	0.39 (4.28)	0.09 (4.45)	0.68 (4.63)	0.00 (4.65)	0.00 (4.65)	0.73 (4.68)
C ₈ H ₁₇ _{inter} ^b	-162.3	-161.7	1.16 (3.95)	0.16 (4.06)	0.03 (4.12)	0.27 (4.18)	0.35 (4.29)	0.11 (4.47)	0.68 (4.64)	0.00 (4.65)	0.00 (4.65)	0.75 (4.71)

a: is a planar Transition State of C₂H₅ with a planar geometry

b: is optimized with a conformation whose tail of the octane interacts with the pi rings

Table S2: R-POCP. Transition natures of the redistributed state S_3 - S_5 with R changing from H to C_2H_5 , the corresponding transition Coefficient and energies (in eV) reported in parenthesis

States	R=H (IO, Cs)	R=H (C_1)	R= CH_3	R= C_2H_5
S_3	$H^a \rightarrow L^b + 2$ (0.47, 4.13 eV)	$H \rightarrow L + 2$ (0.47, 4.15 eV)	$H \rightarrow L + 2$ (0.40, 4.12 eV)	$H \rightarrow L + 2$ (0.38, 4.11 eV) $H \rightarrow L + 4$ (0.31, 4.11 eV)
S_4	$H \rightarrow L + 4$ (0.43, 4.21 eV)	$H \rightarrow L + 4$ (0.45, 4.22 eV)	$H \rightarrow L + 4$ (0.46, 4.17 eV)	$H \rightarrow L + 4$ (0.44, 4.16 eV)
S_5	$H \rightarrow L + 3$ (0.35, 4.30 eV) $H \rightarrow L + 4$ (0.34, 4.30 eV)	$H \rightarrow L + 3$ (0.36, 4.30 eV) $H \rightarrow L + 4$ (0.34, 4.30 eV)	$H - 1 \rightarrow L + 2$ (-0.36, 4.28 eV) $H \rightarrow L + 3$ (0.42, 4.28 eV)	$H - 1 \rightarrow L + 2$ (0.37, 4.28 eV) $H \rightarrow L + 4$ (0.42, 4.28 eV)

a: the highest occupied molecular orbital (HOMO);

b: the lowest unoccupied molecular orbital (LUMO)

Table S3: Et-POCP. Excitation energies E_{gf} (eV), oscillator strengths δ_{OPA} (au) for one-photon absorption, and dominating transition nature for the first 10 lowest excited states of Et-POCP in DMF obtained at CAMB3LYP/6-31G(d,p) level at the geometry optimized at CAMB3LYP/6-31G(d,p) level

State	E_{gf}	δ_{OPA}	Transition	Coefficient
S ₁	3.91	1.24	H→L	0.50
S ₂	4.05	0.17	H-1→L	0.41
			H→L+1	0.44
S ₃	4.11	0.03	H-1→L+2	0.31
			H→L+4	0.38
S ₄	4.16	0.22	H→L+4	0.44
S ₅	4.28	0.35	H-1→+2	-0.37
			H→L+3	0.42
S ₆	4.46	0.11	H-1→L+3	0.31
			H→L+5	0.43
S ₇	4.63	0.66	H-1→L+4	0.48
S ₈	4.65	0.00	H-1→L+5	0.42
			H→L+6	-0.35
S ₉	4.65	0.00	H-7→L	0.38
			H-7→L+1	0.45
S ₁₀	4.69	0.70	H-→L+5	0.38
			H→L+6	0.44

Table S4: H-POCP. Excitation energies E_{gf} (eV) with the symmetric reported in parenthesis, oscillator strength δ_{OPA} (au) and square of transition dipole moments (μ^2) of the first ten excited states, obtained at CAM-B3LYP/6-31G(d,p) level in DMF for the three conformers of H-POCP

Ev	II	IO	OO
S ₁	3.93 (B2)	3.92 (A')	3.92 (B2)
S ₂	4.05 (A1)	4.05 (A')	4.05 (A1)
S ₃	4.14 (B2)	4.13 (A')	4.14 (B2)
S ₄	4.17 (A1)	4.21 (A')	4.20(A1)
S ₅	4.36 (A1)	4.29 (A')	4.27 (A1)
S ₆	4.45 (B2)	4.47 (A')	4.45 (B2)
S ₇	4.62 (B2)	4.64 (A')	4.65 (A2)
S ₈	4.65 (A2)	4.65 (A')	4.65 (B1)
S ₉	4.65 (B1)	4.65 (A')	4.68 (B2)
S ₁₀	4.69 (A1)	4.69 (A')	4.69 (A1)
δ_{OPA}	II	IO	OO
S ₁	1.11	1.24	1.38
S ₂	0.20	0.17	0.16
S ₃	0.098	0.16	0.43
S ₄	0.15	0.19	0.013
S ₅	0.42	0.23	0.062
S ₆	0.16	0.16	0.045
S ₇	0.72	0.57	0
S ₈	0	0	0
S ₉	0	0	0.48
S ₁₀	0.62	0.62	0.62
μ^2	II	IO	OO
S ₁	11.51	12.91	14.39
S ₂	1.96	1.72	1.60
S ₃	0.97	1.55	4.23
S ₄	1.48	1.81	0.13
S ₅	3.89	2.21	0.60
S ₆	1.48	1.42	0.41
S ₇	6.37	5.03	0
S ₈	0	0	0
S ₉	0	0	4.22
S ₁₀	5.45	5.39	5.37

Table S5: H-POCP. Vertical and adiabatic excitation energies E (hartree), solvent reorganization energy λ (eV), as well as oscillator strength δ_{OPA} (au) for the first six excited states, computed with the state-specific (SS) implementation of PCM at CAM-B3LYP/6-31G(d,p) level in DMF for three carbazole analogue IO, II, OO

States	ES (neq)	ES (eq)	λ (eV)	δ_{OPA} (neq)	δ_{OPA} (eq)
IO					
S ₁	-1952.46908693	-1952.48350591	0.3924	0.9009	0.3146
S ₂	-1952.46832654	-1952.48351043	0.4132	0.0849	0.3145
S ₃	-1952.46142711	-1952.46492751	0.0953	0.2648	0.3745
S ₄	-1952.45625271	-1952.45695783	0.0192	0.1494	0.1382
S ₅	-1952.45437828	-1952.45552028	0.0311	0.1432	0.1106
S ₆	-1952.45187698	-1952.45496845	0.0841	0.1302	0.1705
II					
S ₁	-1952.46880593	-1952.47271717	0.1064	0.8406	0.6872
S ₂	-1952.46809242	-1952.47428660	0.1686	0.0731	0.0559
S ₃	-1952.46121259	-1952.46505528	0.1046	0.1939	0.2362
S ₄	-1952.45688896	-1952.45735588	0.0127	0.0891	0.094
S ₅	-1952.45179985	-1952.45251043	0.0193	0.2492	0.2289
S ₆	-1952.45132097	-1952.45415209	0.0770	0.1346	0.2215
OO					
S ₁	-1952.46880593	-1952.47271717	0.1064	0.9524	0.7270
S ₂	-1952.46809242	-1952.47428660	0.1686	0.0891	0.0863
S ₃	-1952.46121259	-1952.46505528	0.1046	0.5509	0.6844
S ₄	-1952.45688896	-1952.45735588	0.0127	0.0103	0.0164
S ₅	-1952.45179985	-1952.45251043	0.0193	0.0423	0.0345
S ₆	-1952.45132097	-1952.45415209	0.0770	0.0689	0.0857

Table S6: H-POCP. Transition dipole derivatives (for transitions $S_0 \rightarrow S_k$, $k=1-6$, in atomic units) along the normal modes that result in a large HT contribution to the spectrum intensity. The frequency associated to the normal mode is given in parenthesis. The modes correspond to the diagonalization of the final state (from VH calculations).

k (freq, cm ⁻¹)	$\left(\frac{\partial \mu_x^{if}}{\partial Q_k}\right)$	$\left(\frac{\partial \mu_y^{if}}{\partial Q_k}\right)$	$\left(\frac{\partial \mu_z^{if}}{\partial Q_k}\right)$	Module
IO_ $S_0 \rightarrow S_1$				
1 (1846i)	1.2361	-0.9781	0.0000	1.5763
IO_ $S_0 \rightarrow S_2$				
1 (1051i)	-1.9556	-2.0237	0.0000	2.8142
175 (2435)	-1.6903	-2.0294	0.0000	2.6411
IO_ $S_0 \rightarrow S_3$				
1 (1119i)	0.3867	-2.2515	0.0000	2.2844
175 (2507)	1.0456	-0.3812	0.0000	1.1130
174 (1943)	-0.3147	-0.9521	0.0000	1.0027
IO_ $S_0 \rightarrow S_4$				
1(671i)	-1.8511	1.0042	0.0000	2.1059
175 (2196)	-1.3048	-0.3255	0.0000	1.3448
IO_ $S_0 \rightarrow S_5$				
174 (2154)	-0.6653	-1.1123	0.0000	1.2960
175 (2383)	-0.0352	0.8184	0.0000	0.8192
91 (941)	-0.0687	-0.6537	0.0000	0.6573
28 (366)	-0.0230	-0.6307	0.0000	0.6311
76 (812)	0.0263	0.6275	0.0003	0.6280
IO_ $S_0 \rightarrow S_6$				
1 (48i)	3.1751	-1.0153	-0.0001	3.3335
28 (352)	1.2542	-0.3209	0.0000	1.2947
46 (513)	0.8336	-0.2616	0.0000	0.8737
175 (2067)	-0.7453	0.4473	0.0000	0.8692
5 (49)	-0.7622	0.2610	0.0000	0.8057
20 (238)	-0.6101	0.1922	0.0000	0.6396
12 (103)	0.6002	-0.1668	0.0000	0.6229
39 (454)	0.4853	-0.1947	0.0000	0.5229
II_ $S_0 \rightarrow S_1$				
1 (1985i)	0.0000	0.0000	1.7589	1.7589
II_ $S_0 \rightarrow S_2$				
175 (2594)	0.0000	-2.4845	0.0000	2.4845
1 (941i)	0.0000	-2.1305	0.0000	2.1305
II_ $S_0 \rightarrow S_3$				
1 (3513i)	0.0000	0.0000	-3.5275	3.5275
174 (2023)	0.0000	1.1031	0.0000	1.1031
175 (2356)	0.0000	0.0000	-1.0653	1.0653

II_S ₀ →S ₄				
196 (4145)	0.0000	2.3829		2.3829
28 (358)	0.0000	0.0000	- 1.0774	1.0774
46 (506)	0.0001	0.0000	- 0.9222	0.9222
21(241)	0.0000	0.0000	- 0.8346	0.8346
51 (575)	0.0001	0.0000	0.7785	0.7785
74 (776)	0.0001	0.0000	0.5476	0.5476
II_S ₀ →S ₅				
1 (454i)	0.0000	-2.4557	0.0000	2.4557
174 (1900)	0.0000	-0.9572	0.0000	0.9572
47(532)	0.0000	-0.9144	0.0000	0.9144
69 (746)	0.0000	-0.6605	0.0000	0.6605
II_S ₀ →S ₆				
24 (294)	0.0000	1.7346	0.0000	1.7346
175 (2227)	0.0000	-1.3373	0.0000	1.3373
21 (243)	- 0.9630	0.0000	0.0001	0.9630
51 (563)	- 0.8931	0.0000	0.0001	0.8931
47 (523)	- 0.8248	0.0000	0.0000	0.8248
54 (580)	0.0000	-0.0002	- 0.7990	0.7990
23 (271)	0.0000	- 0.7601	0.0000	0.7601
13 (152)	0.0000	0.0000	0.7001	0.7001
67 (726)	0.0001	0.0000	0.6392	0.6392
48 (548)	0.0000	-0.0001	0.5851	0.5851
63 (713)	0.0000	0.0000	0.5380	0.5380
OO_S ₀ →S ₁				
1 (1840i)	0.0000	0.0000	-1.4515	1.4515
58 (646)	0.0000	0.6109	0.0000	0.6109
75 (779)	0.0000	0.5765	0.0000	0.5765
87 (878)	0.0000	0.5723	0.0000	0.5723
61 (659)	0.0000	0.5246	0.0000	0.5246
OO_S ₀ →S ₂				
1(960i)	0.0000	3.6808	0.0000	3.6808
175 (2048)	0.0000	-3.0225	0.0000	3.0225
45 (501)	0.0000	0.6720	0.0000	0.6720
OO_S ₀ →S ₃				
1 (1260i)	0.0000	0.0000	1.0889	1.0889
174 (2030)	0.0000	-1.0358	0.0000	1.0358
175 (2479)	0.0000	-0.1729	0.0000	0.1729
OO_S ₀ →S ₄				
175 (1844)	0.0000	1.0564	0.0000	1.0564
OO_S ₀ →S ₅				
175 (2554)	0.0000	-1.7001	0.0000	1.7001
OO_S ₀ →S ₆				
5	0.0000	-0.0001	3.2694	3.2694

28	0.0000	0.0000	1.6389	1.6389
4	0.0000	0.0000	- 0.9528	0.9528
45	0.0000	0.0000	- 0.8080	0.8080
175	0.0000	0.0000	0.7695	0.7695
38	0.0000	0.0000	- 0.7670	0.7670
21	0.0000	-0.0001	- 0.7520	0.7520
42	0.0000	0.0000	0.6046	0.6046

Note: due to strong Duschinsky mixings, it is not always possible to establish a one-to-one correspondence between these excited-state modes and the ground-state modes shown in Fig. 11.

Table S7: H-POCP. Projection over the transition dipole moments of the transition dipole derivatives (for transitions $S_0 \rightarrow S_k$, $k=1-6$) along the normal modes that result in a large HT contribution to the spectrum intensity for II and OO. The frequency associated to the normal mode is given in parenthesis. For each transition the modes correspond to the diagonalization of the final state Hessian. (highlighted the terms that are connected with the couplings indicated in Table 3, in blue for the state above, and in red with the state below)

Projection on (II)						
K (freq, cm^{-1})	$\mu_{S_0-S_1}$	$\mu_{S_0-S_2}$	$\mu_{S_0-S_3}$	$\mu_{S_0-S_4}$	$\mu_{S_0-S_5}$	$\mu_{S_0-S_6}$
$S_0 \rightarrow S_1$						
1_1 (1985i)	0.00	1.00	0.00	1.00	1.00	0.00
$S_0 \rightarrow S_2$						
175_2 (2594)	-1.00	0.00	-1.00	0.00	0.00	-1.00
1_2 (941i)	-1.00	0.00	-1.00	0.00	0.00	-1.00
$S_0 \rightarrow S_3$						
1_3 (3513i)	0.00	1.00	0.00	1.00	1.00	0.00
174_3 (2023)	1.00	0.00	1.00	0.00	0.00	1.00
175_3 (2356)	0.00	-1.00	0.00	-1.00	-1.00	0.00
$S_0 \rightarrow S_4$						
196_4 (4145)	-1.00	0.00	-1.00	0.00	0.00	-1.00
28_4 (358)	0.00	-1.00	0.00	-1.00	-1.00	0.00
46_4 (506)	0.00	1.00	0.00	1.00	1.00	0.00
$S_0 \rightarrow S_5$						
1_5 (454i)	-1.00	0.00	-1.00	0.00	0.00	-1.00
174_5 (1900)	1.00	0.00	1.00	0.00	0.00	1.00
47_5 (532)	1.00	0.00	1.00	0.00	0.00	1.00
$S_0 \rightarrow S_6$						
24_6 (294)	-1.00	0.00	-1.00	0.00	0.00	-1.00
175_6 (2226)	0.00	1.00	0.00	1.00	1.00	0.00
21_6 (243)	1.00	0.00	1.00	0.00	0.00	1.00
Projection on (OO)						
K (freq, cm^{-1})	$\mu_{S_0-S_1}$	$\mu_{S_0-S_2}$	$\mu_{S_0-S_3}$	$\mu_{S_0-S_4}$	$\mu_{S_0-S_5}$	$\mu_{S_0-S_6}$
$S_0 \rightarrow S_1$						
1_1 (1840i)	0.00	-1.00	0.00	1.00	-1.00	0.00

$S_0 \rightarrow S_2$						
1_2 (960i)	-1.00	0.00	-1.00	0.00	0.00	-1.00
175_2 (2407)	1.00	0.00	1.00	0.00	0.00	1.00
$S_0 \rightarrow S_3$						
1_3 (1260i)	0.00	-1.00	0.00	1.00	-1.00	0.00
174_3 (2030)	1.00	0.00	1.00	0.00	0.00	1.00
175_3 (2479)	0.00	-1.00	0.00	1.00	-1.00	0.00
$S_0 \rightarrow S_4$						
175_4 (1844)	-1.00	0.00	-1.00	0.00	0.00	-1.00
$S_0 \rightarrow S_5$						
175_5 (2554)	1.00	0.00	1.00	0.00	0.00	1.00
$S_0 \rightarrow S_6$						
5_6 (83)	-1.00	0.00	-1.00	0.00	0.00	-1.00
28_6 (396)	0.00	1.00	0.00	1.00	1.00	0.00
4_6 (51)	1.00	0.00	1.00	0.00	0.00	1.00